

Theory of fractional Knight shift in liquid binary alloys

P. Jena

Physics Department, Virginia Commonwealth University, Richmond, Virginia 23284

G. B. Taggart

The BDM Corporation, 7915 Jones Branch Drive, McLean, Virginia 22102

B. K. Rao*

Physics Department, Virginia Commonwealth University, Richmond, Virginia 23284

(Received 29 May 1984)

A theory, based on the density-functional formalism, is developed to calculate the fractional change in the Knight shift of a liquid metal due to dilute impurities. The spin densities around the impurities are calculated self-consistently using the local-density approximation. The disorder in the liquid state is taken into account by incorporating into the theory the pair-correlation function of the host metal. In the numerical computation, both the experimental and model pair-correlation functions are used. The present formulation takes into account the magnetic-field-induced distortion of the conduction-electron states both at and below the Fermi energy and is valid at any distance from the impurity. The theory is applied to liquid Al alloys containing Mg, Si, Ga, and Ge impurities. The results are compared with the predictions of an asymptotic model based on the conventional expression for the Knight shift. The results are in reasonable agreement with experiment; however, additional theoretical and experimental work is called for. The theory is applicable to other disordered systems such as amorphous alloys.

I. INTRODUCTION

Thirty-five years ago Knight¹ observed a shift in the resonance frequency of ⁶³Cu in metallic copper from that in diamagnetic CuCl. This shift, now termed the Knight shift, was later shown to be a characteristic property of the metal and arises from the interaction of the nuclear magnetic moment with conduction-electron spins polarized by the external magnetic field. Assuming that this interaction is dominated by the Fermi contact term, Townes *et al.*² derived a simple expression for the Knight shift, namely,

$$K = \frac{8\pi}{3} \chi_s \langle |\psi_{k_F}(0)|^2 \rangle_{av},$$

where $\langle |\psi_{k_F}(0)|^2 \rangle_{av}$ is the density of conduction electrons at the probe nucleus averaged over the Fermi surface and χ_s is the Pauli spin susceptibility. The calculation of the conduction-electron density in a perfect metal requires a detailed knowledge of the band structure. An accurate determination of the spin susceptibility, on the other hand, depends on how well one understands the many-body effects associated with the interacting electrons. It is due to these reasons that a quantitative theory for the Knight shift in perfect metals has been difficult to develop.

In imperfect metals, there are other problems that hinder both experimental and theoretical investigations. For example, the presence of impurities and imperfections causes perturbations on the spatial distribution of conduction-electron densities in the material. As a result,

the host-resonating nuclei experience different local fields and resonate at different frequencies. This gives rise to either a broadening or a further shift in the nuclear resonance frequency. This additional shift in the resonance frequency, which is characteristic of the impurity in a given host, is difficult to obtain experimentally. This is particularly the case when the additional fractional shift is small in magnitude.

From a theoretical point of view, the perturbations on the conduction-electron states are difficult to calculate quantitatively due to the loss in the periodicity of the crystal. Recent methods,³ based on a Green's-function approach, have permitted one to obtain a semiquantitative understanding of the conduction-electron states by confining the perturbation within a muffin-tin cell around the impurity and matching the solution to the host Green's function outside the cell. For a disordered material such as amorphous and liquid metals the common methods usually employed are based upon the coherent-potential approximation.⁴ It would, thus, appear that a quantitative theoretical treatment of the electronic structure of impurities in a disordered metal is a very difficult task since imperfections are introduced not only by the structural disorder, but also by the impurities.

As was pointed out by Ashcroft and Lekner,⁵ the loss of long range order in the liquid state may have an added advantage for electronic structure calculations in liquid metals. This is because the electrons can be treated as free-electron-like and this approximation is expected to be more valid for metals in the liquid phase than in the solid state. In this paper we extend the free-electron treatment to liquid binary alloys. We treat the host liquid metal as a

free-electron system. The perturbation on the host electron density for both spin orientations due to the impurity atom is calculated self-consistently using spin-density-functional formalism.⁶ The induced spin density around the impurity atom exhibits the well-known Friedel oscillations at the asymptotic region. Thus the net spin density at a near-neighbor host atom may either be enhanced or diminished depending on its distance from the impurity atom and the phase of the spin-density oscillations. This would induce a corresponding change in the local field and resonance frequency of the host atoms. A configuration average of these changes leads to the determination of the fractional Knight shift. The theory developed here is applicable to free-electron-like liquid metals in general. We have applied it to study the fractional change in the Knight shift in liquid Al due to Mg, Si, Ga, and Ge impurities in the dilute limit.

In the next section we outline our theoretical approach and compare it to earlier theoretical attempts^{7,8} for calculating Knight shifts in liquid binary alloys. In Sec. III the electronic structure of binary liquid alloys and Knight-shift results are compared with experimental values. We also discuss the importance of mechanisms other than the Fermi contact term in the calculations of Knight shifts and reasons for the remaining disagreement between theory and experiment.⁷

II. THEORETICAL FORMULATION

The hyperfine (hf) field at a nuclear site due to the contact interaction between the nuclear magnetic moment and spin-polarized electrons is given by

$$B_{\text{hf}} = \frac{8\pi}{3} \mu_B [n^\uparrow(0) - n^\downarrow(0)], \quad (1)$$

where $n^\uparrow(0)$ and $n^\downarrow(0)$ are, respectively, the density of spin-up and spin-down electrons at the nuclear site. The Knight shift is then given by

$$K = \frac{B_{\text{hf}}}{B_{\text{ext}}} \frac{8\pi}{3} \chi_s \left[\frac{n^\uparrow(0) - n^\downarrow(0)}{n_0^\uparrow - n_0^\downarrow} \right], \quad (2)$$

where $n_0^\uparrow - n_0^\downarrow$ is the ambient spin density of the conduction electrons caused by the external magnetic field, B_{ext} . It has been shown by Munjal and Petzinger⁹ that Eq. (2) leads to the conventional form

$$K = \frac{8\pi}{3} \chi_s \langle |\psi_{k_F}(0)|^2 \rangle_{\text{av}} \quad (3)$$

when the scattering is limited to the Fermi-surface electrons with wave number k_F only. Equation (3), therefore, ignores the effect of the magnetic field on the electrons below the Fermi surface and is an approximate form of Eq. (2).

In a perfect metal, the Knight shift at any nuclear site is identical to that at any other nuclear site. Thus the average Knight shift, K_0 , per atom in a perfect host,

$$K_0 = \frac{1}{N} \sum_{\nu} K_0(\vec{R}_{\nu}), \quad (4)$$

is identical with $K_0(\vec{R}_{\nu})$. In Eq. (4), N denotes the number of atoms in the sample and the subscript 0 denotes

that quantities are for a perfect host. When an impurity is introduced, the conduction electrons around the impurity are perturbed. This perturbation, in the asymptotic region, leads to the Friedel oscillations in the charge and spin density. Since the induced spin density $n^\uparrow(r) - n^\downarrow(r)$ is spatially varying, the contact spin density at any host nuclear site would depend upon the distance between the host and impurity atom. Thus the average Knight shift, \bar{K} , per atom in the imperfect system, is given by

$$\bar{K} = \frac{1}{N} \sum_{\nu} K(\vec{R}_{\nu}), \quad (5)$$

where $K(\vec{R}_{\nu})$ is the Knight shift at the host atom site at a distance \vec{R}_{ν} from the impurity. In Eq. (5), the summation excludes the atom at the origin which is occupied by the impurity. The change in the average Knight shift due to the impurity is then

$$\Delta\bar{K} = \bar{K} - \bar{K}_0 = \frac{1}{N} \left[\sum_{\nu} K(\vec{R}_{\nu}) - \sum_{\nu} K_0(\vec{R}_{\nu}) \right], \quad (6)$$

writing

$$K(\vec{R}_{\nu}) = K_0(\vec{R}_{\nu}) + \Delta K(\vec{R}_{\nu}), \quad (7)$$

Eq. (6) becomes (in the limit N is large)

$$\Delta\bar{K} = \frac{1}{N} \sum_{\nu} \Delta K(\vec{R}_{\nu}). \quad (8)$$

For the fractional change in the Knight shift for concentration c of the impurity, we have

$$\Gamma \equiv \frac{1}{c} \frac{\Delta\bar{K}}{\bar{K}} = \sum_{\nu} \Delta K(\vec{R}_{\nu}) / K_0. \quad (9)$$

Using Eq. (2) in Eq. (9), we have

$$\Gamma = \sum_{\nu} \Delta n(\vec{R}_{\nu}) / [n^\uparrow(0) - n^\downarrow(0)], \quad (10)$$

where

$$n^\sigma(\vec{R}_{\nu}) = n_0^\sigma(\vec{R}_{\nu}) + \delta n^\sigma(\vec{R}_{\nu})$$

and

$$\Delta n(\vec{R}_{\nu}) = \delta n^\uparrow(\vec{R}_{\nu}) - \delta n^\downarrow(\vec{R}_{\nu}). \quad (11)$$

In Eq. (11) $n^\sigma(n_0^\sigma)$ is the density of the electrons with spin σ (\uparrow or \downarrow) at site \vec{R}_{ν} in the imperfect (perfect) system, and δn^σ is the perturbation produced by the impurity at a distance R_{ν} . $\Delta n(\vec{R}_{\nu})$ is then the perturbed spin density. In an all-electron calculation, Eq. (10) would include the orthogonalization of perturbed conduction electrons to the host core orbital. In a pseudopotential calculation, on the other hand, the core electrons are frozen and the effect of orthogonality of conduction electrons with core orbitals on the Knight shift manifests itself in an enhancement factor, α . Rigney and Flynn⁷ have shown that in an alloy system such a procedure can also be followed. Thus we can write

$$\Delta n(\vec{R}_{\nu}) \simeq \alpha \Delta \tilde{n}(\vec{R}_{\nu}) \quad (12a)$$

and

$$n^\uparrow(0) - n^\downarrow(0) \simeq \alpha(n_0^\uparrow - n_0^\downarrow). \quad (12b)$$

Substituting Eq. (12) in Eq. (10), we have

$$\Gamma = \sum'_v \left[\frac{\Delta \tilde{n}(\vec{R}_v)}{n_0^\uparrow - n_0^\downarrow} \right]. \quad (13)$$

$\Delta \tilde{n}(\vec{R}_v)$ in Eq. (12) is the spin-density distribution around an impurity embedded in a free-electron gas and can be calculated self-consistently in the density-functional formulation using the jellium model.¹⁰

In a liquid metal, the atoms are in a disordered state. The summation in Eq. (13) over nuclear positions can be carried out by performing the following integration:

$$\Gamma = \int d^3r \rho(r) \left[\frac{\Delta \tilde{n}(r)}{n_0^\uparrow - n_0^\downarrow} \right], \quad (14)$$

where

$$\rho(r) = \frac{1}{\Omega_0} g(r). \quad (15)$$

$g(r)$ is the conventional pair-correlation function and Ω_0 is the atomic volume. $g(r)$ can be determined from experimental structure-factor data¹¹ or from model calculations.⁵ In Eq. (14), the induced spin density in the large parentheses decreases as $1/r^3$ modulated by a sinusoidal function at large r . Thus the integrand in Eq. (14) decreases as $1/r$ modulated by the sinusoidal function. At small r , while the induced spin density is large, the number of host atoms contributing to the fractional Knight shift in Eq. (14) is small. On the other hand, at large r , the number of atoms is large while the induced spin density is small. Consequently, the contribution to the fractional Knight shift from atoms close to the impurity may be as large as those further away. Thus it is important to calculate an induced spin density that is valid at all distances from the impurity.

In the following we describe briefly the density-functional approach that we have used to calculate the induced spin density. The problem reduces to solving the Hohenberg-Kohn-Sham equations,⁶

$$[-\nabla^2 + V_{\text{eff}}^\sigma(\vec{r})] \psi_k^\sigma(\vec{r}) = \epsilon_k^\sigma \psi_k^\sigma(\vec{r}), \quad (16)$$

We have used atomic units ($\hbar=1$, $m=1/2$, $e^2=2$). The effective potential, V_{eff}^σ , is assumed to be spherically symmetric. Thus Eq. (16) reduces to a one-dimensional equation

$$\left[-\frac{d^2}{dr^2} + \frac{l(l+1)}{r^2} + V_{\text{eff}}^\sigma(r) \right] R_{kl}^\sigma(r) = (k^\sigma)^2 R_{kl}^\sigma(r), \quad (17)$$

where the one-particle wave function

$$\psi_k^\sigma(\vec{r}) = \sum_{lm} R_{kl}^\sigma(r) Y_{lm}(\hat{r}). \quad (18)$$

k^σ is the wave vector for an electron with spin σ (\uparrow or \downarrow). The effective potential is given by

$$V_{\text{eff}}^\sigma = V_{\text{es}} + V_{\text{xc}}^\sigma, \quad (19)$$

where V_{xc}^σ is the exchange-correlation potential¹² in the local-density approximation and is defined with respect to the ambient environment. The electrostatic potential is obtained by solving Poisson's equation

$$\nabla^2 V_{\text{es}}(r) = -8\pi[n_{\text{ext}} - n(r)], \quad (20)$$

where the electron density $n(r)$ is given by

$$n(r) = \sum_k^{\text{occ}} [|\psi_k^\uparrow(r)|^2 + |\psi_k^\downarrow(r)|^2]. \quad (21)$$

The external perturbation is assumed to have the form

$$n_{\text{ext}}(\vec{r}) = A \delta(\vec{r}) + n_0 \Theta(\vec{r} - \vec{R}_{\text{ws}}) \quad (22)$$

[WS represents a Wigner-Seitz cell]. Here A is the atomic number of the host and/or impurity atom, n_0 is the average density of electrons and/or positive ions in the unperturbed host, and Θ is the usual Heaviside unit-step function. Equations (16)–(22) are solved self-consistently.

To compute the fractional Knight shift in Eq. (14), we solve Eqs. (16)–(22) self-consistently for both the host and impurity atoms. This is done by using A equal to an atomic number of the host and calculating the induced spin density around the host atoms. The calculation is then repeated for the impurity. The difference between the spin densities around impurity and host atoms then enters into the calculation of the fractional Knight shift.

It is now possible to derive a simple analytic expression for the Knight shift valid at the asymptotic region. In this limit the radial wave function $R_{k_{F_l}}(r)$ for the Fermi-surface electrons can be expressed as

$$R_{k_{F_l}}(r) = \cos \delta_l(\epsilon_F) j_l(k_F r) - \sin \delta_l(\epsilon_F) n_l(k_F r) \quad \text{as } r \rightarrow \infty, \quad (23)$$

where $\delta_l(\epsilon_F)$ is the scattering phase shift for the l th partial wave at energy ϵ_F , and j_l and n_l are spherical Bessel and Neuman functions. It is straightforward to show that in the asymptotic limit

$$|\psi_{k_F}(r)|^2 = \sum_l (2l+1) [\cos \delta_l(\epsilon_F) j_l(k_F r) - \sin \delta_l(\epsilon_F) n_l(k_F r)]^2. \quad (24)$$

Using the conventional expression (3), the fractional Knight shift is

$$\Gamma = \int d^3r \rho(r) \left[\frac{|\psi_{k_F}(r)|^2 - |\psi_{k_F}^{(0)}(r)|^2}{|\psi_{k_F}^{(0)}(r)|^2} \right], \quad (25)$$

where $\psi_{k_F}^{(0)}(r) = e^{i\vec{k}_F \cdot \vec{r}}$ is the unperturbed wave function of the Fermi-surface electron of the perfect host. It is easy to show that

$$|\psi_{k_F}^{(0)}(r)|^2 = 1 = \sum_{l=0}^{\infty} (2l+1) j_l^2(k_F r). \quad (26)$$

Using Eqs. (26) and (24) in Eq. (25), we obtain

$$\Gamma = \int d^3r \rho(r) \left[\sum_l (2l+1) [n_l^2(\mu_{FR}) - j_l^2(k_{FR})] \sin^2 \delta_l(\epsilon_F) - \sum_l (2l+1) n_l(k_{FR}) j_l(k_{FR}) \sin 2\delta_l(\epsilon_F) \right]. \quad (27)$$

Rigney and Flynn⁷ have recast Eq. (27) in the form

$$\Gamma = \sum_l \{ A_l \sin^2 \delta_l(\epsilon_F) + B_l \sin[2\delta_l(\epsilon_F)] \}, \quad (28)$$

where

$$A_l \equiv (2l+1) \int d^3r \rho(r) [n_l^2(k_{FR}) - j_l^2(k_{FR})], \quad (29)$$

$$B_l \equiv -(2l+1) \int d^3r \rho(r) n_l(k_{FR}) j_l(k_{FR}).$$

Thus A_l and B_l are quantities that depend upon the properties of the perfect host metal and can be determined finally. The fractional Knight-shift calculation in Eq. (28) needs only the scattering phase shift and can be used to study various impurity systems with ease. However, as shown in the Appendix, this procedure leads to inaccurate results since numerical evaluation of the A_l 's and B_l 's in Eq. (29) is difficult. Thus it is necessary to evaluate Eq. (27) directly.

Recently Iwamatsu *et al.*⁸ have calculated the Knight shifts for liquid binary alloys of simple metals using a pseudopotential procedure and the conventional expression for the Knight shift. This method, although simpler than our density-functional scheme, suffers not only from the ambiguity associated with pseudopotentials, but also that it makes use of a low-order perturbation theory.

III. RESULTS AND DISCUSSION

We now present the results of the spin-density distribution around both host and impurity atoms calculated in the density-functional theory. In order to calculate $n^\sigma(r)$, we initially polarized the electron gas by choosing

$$(n_0^\uparrow - n_0^\downarrow)/n_0 = 0.1. \quad (30)$$

The induced polarization $n^\uparrow(r) - n^\downarrow(r)$ is proportional to the ambient polarization $(n_0^\uparrow - n_0^\downarrow)$ in this limit. Thus the Knight shift in Eq. (14) is independent of the choice of this ambient polarization.

In Fig. 1 we plot the spin density $n^\uparrow(r) - n^\downarrow(r)$ around an Al nucleus embedded inside a vacancy in a homogeneous electron gas¹³ of density given by $r_s = 2.17$, appropriate to liquid Al at the melting temperature. Figure 1 shows the spin density for distances that are relevant to the calculation of the Knight shift. The pair-distribution function, as described later, has the first peak around $5a_0$, which is also very close to the hard-sphere diameter of $4.8a_0$. Thus the contribution to the integrand in Eq. (14) is nonvanishing for $r > 4.8a_0$. Figure 1 also exhibits the well-known Friedel oscillations which asymptotically approach the ambient spin-polarized density.

The calculations of the spin density around the substitutional impurities ^{12}Mg , ^{31}Ga , ^{14}Si , and ^{32}Ge were repeated by using the appropriate atomic numbers in Eq. (22) and carrying out the density-functional calculations to full self-consistency. For ^{12}Mg , ^{13}Al , and ^{14}Si , the solutions led to bound electrons in $1s^2$, $2s^2$, $2p^6$ orbits. The num-

ber of electrons in the scattering state, and thus the valence Z of ^{12}Mg , ^{13}Al , and ^{14}Si were found to be 2, 3, and 4, respectively. For ^{31}Ga and ^{32}Ge we found bound states in $1s^2$, $2s^2$, $2p^6$, $3s^2$, $3p^6$, and $3d^{10}$ states. The valence Z of ^{31}Ga and ^{32}Ge are, respectively, 3 and 4. The valence difference between impurity and host, $\Delta Z = Z_I - Z_H$ is -1 for ^{12}Mg , 0 for ^{31}Ga , and $+1$ for ^{32}Ge and ^{14}Si .

In Fig. 2 we have plotted the difference in the spin density between the impurity (Mg, Ga) and host atom, i.e.,

$$\Delta \tilde{n}(r) = [n^\uparrow(r) - n^\downarrow(r)]_{\text{impurity}} - [n^\uparrow(r) - n^\downarrow(r)]_{\text{host}}, \quad (31)$$

since it is this quantity that enters into the calculation of the fractional Knight shift in Eq. (14). It is clear from Fig. 2 that the induced perturbation around ^{12}Mg is larger than that around ^{32}Ga . Two main conclusions can be made from Fig. 2. First, ^{13}Al and ^{31}Ga , although having the same valence structure, have different core-electronic structure. That $\Delta \tilde{n}(r)$ for Al/Ga is finite indicates that for isovalent atoms, the core structure plays a role in perturbing the ambient environment of the host. For ^{12}Mg and ^{13}Al , on the other hand, the core-electronic structure is the same while the valence structure is not. Since ^{12}Mg is found to provide a larger perturbation than ^{31}Ga on the ambient spin distribution in ^{14}Al , one can conclude that valence difference between impurity and host atom plays a larger role in perturbing the ambient environment than the difference in the core-electronic structure.

In Fig. 3 we plot the induced spin density around ^{32}Ge and ^{14}Si . For both impurities in ^{13}Al , $Z = +1$. Yet ^{32}Ge provides a larger perturbation on the host than ^{14}Si . This supports our discussion above that the core-electronic structure plays a role in the perturbation. The perturbations exhibited in Figs. 2 and 3 have a direct effect on the fractional Knight shift.

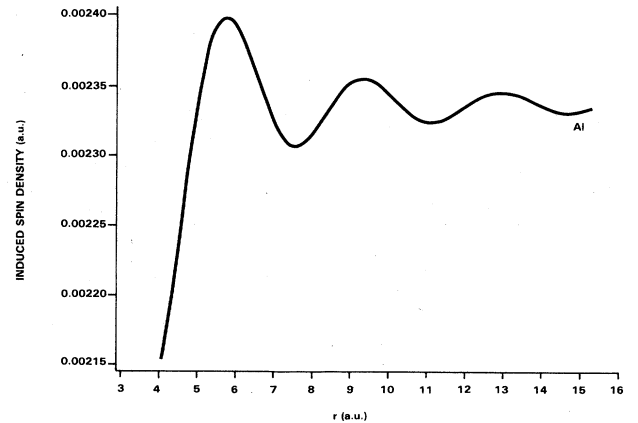


FIG. 1. Induced spin-density distribution $n^\uparrow(r) - n^\downarrow(r)$ around an Al nucleus embedded in a vacancy site in liquid Al.

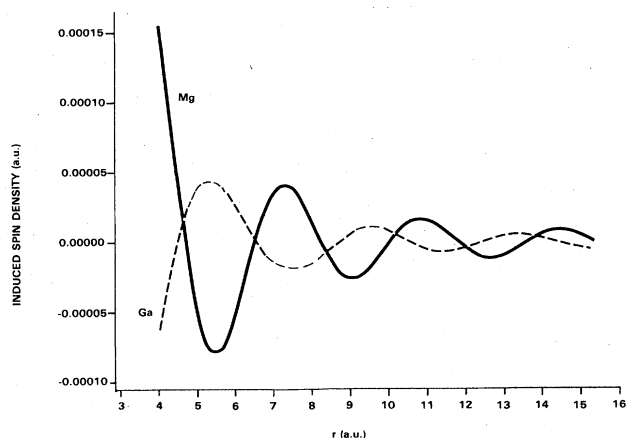


FIG. 2. Induced spin density $\Delta\bar{n}(r)=[n^{\uparrow}(r)-n^{\downarrow}(r)]_{\text{imp}} - [n^{\uparrow}(r)-n^{\downarrow}(r)]_{\text{host}}$ around Mg (solid line) and Ga (dashed line) in liquid Al.

Before presenting the calculations of the Knight shift, we would like to discuss the pair-correlation function $g(r)$ in the liquid host, since it is needed for the evaluation of the Knight shift. The pair-correlation function is obtained by Fourier transforming the interference function of the liquid metal. This transform often introduces errors in the pair-correlation function associated with the truncation in the diffracted intensity at a certain wave number. The possible errors in the data analysis and data reduction have been discussed by Fessler *et al.*¹¹ in detail. In Fig. 4 we show the experimental $g(r)$ obtained from x-ray diffraction studies by Fessler *et al.*¹¹ We have compared this $g(r)$ with the hard-sphere model⁵ based on the Percus-Yevick equation. We have used a packing density of $\eta=0.46$ for our calculation. The agreement with experiment is excellent beyond the first peak. The difference between the model and experimental $g(r)$ around the first peak is insignificant so far as the calculation of the fractional Knight shift is concerned.

In Table I we compare the fractional Knight shift calculated using the density-functional result [Eq. (14)] and

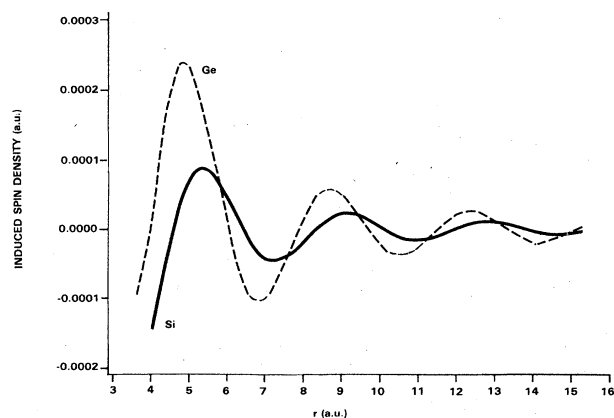


FIG. 3. Induced spin density $\Delta\bar{n}(r)=[n^{\uparrow}(r)-n^{\downarrow}(r)]_{\text{imp}} - [n^{\uparrow}(r)-n^{\downarrow}(r)]_{\text{host}}$ around Si (solid line) and Ge (dashed line) in liquid Al.

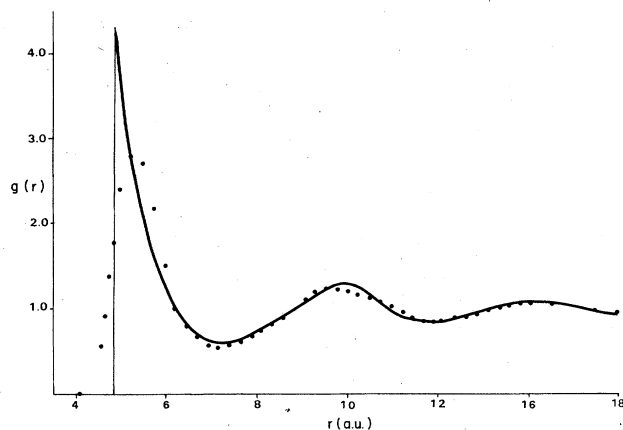


FIG. 4. Pair-distribution function $g(r)$ in liquid Al. The solid line is calculated using the hard-sphere model (Ref. 12). The dotted curve represents the experimental $g(r)$ (Ref. 11).

the asymptotic formula [Eq. (27)] with experiment. We should point out that the partial-wave phase shifts used in the asymptotic formula in Eq. (27) were obtained from our density-functional calculations. The summation over l was carried up to $l=10$. The reader is referred to the Appendix where we discuss the numerical procedure and the necessity for using Eq. (27) over Eq. (28) and for retaining higher values of l in the partial-wave sum.

The agreement between the asymptotic and nonasymptotic values of the Knight shift in Al/Si and Al/Ga is satisfactory while for Al/Mg and Al/Ge the values differ by a factor of 2. This shows that the asymptotic formula for the Knight shift is not valid in general and that the contribution of near-neighbor atoms to the fractional Knight shift may be quite important. For near-neighbor sites, the asymptotic expression is not valid.

We now compare the density-functional result with experiment. Except in the case of Al/Ga the agreement with experiment is fairly poor. Of particular interest to note is Al/Mg where the sign of the calculated fractional Knight shift is opposite to that in experiment. This disagreement is unsettling, since liquid metals, such as Al, are ordinarily characterized as free-electron-like where Ziman's¹⁴ theory applies.

TABLE I. Comparison between fractional Knight shifts $\Gamma=K^{-1}\partial K/\partial c$ due to ^{12}Mg , ^{14}Si , ^{31}Ga , and ^{32}Ge obtained from experiment, self-consistent spin-density-functional, and phase-shift (asymptotic) calculations.

Impurity	Knight shift in liquid Al alloys		
	Experiment	Density functional	Phase shift
^{12}Mg	0.01	-0.23	-0.11
^{14}Si	0.07	0.29	0.23
^{31}Ga	0.14	0.16	0.13
^{32}Ge	0.21	0.44	0.70

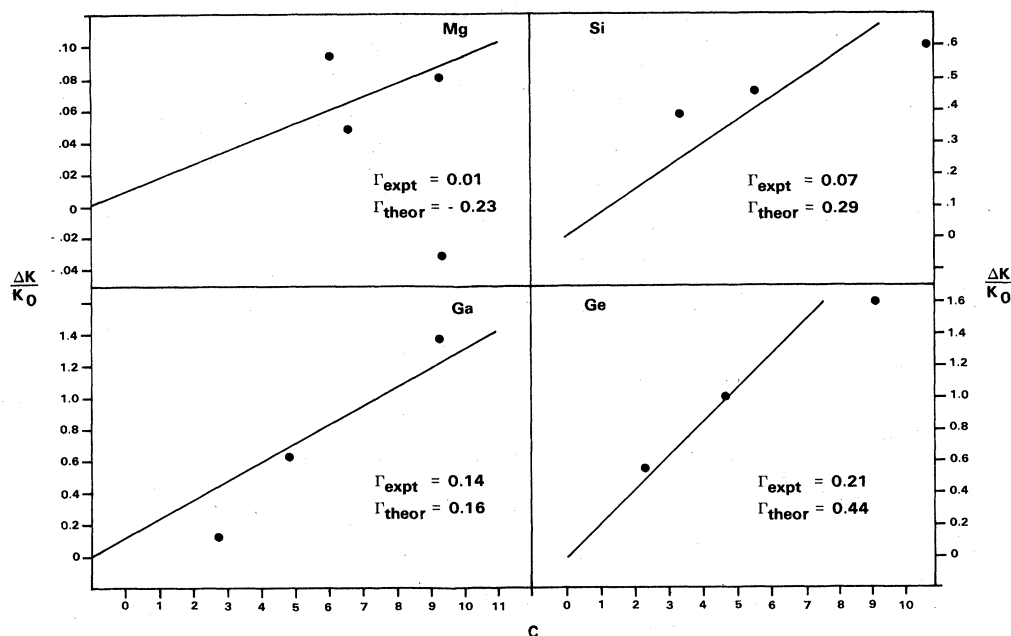


FIG. 5. Experimental data points from which the experimental fractional Knight shift $\Gamma = K^{-1} \partial K / \partial c$ was obtained by Rigney and Flynn (Ref. 7). The straight line corresponds to the Γ values quoted by Rigney and Flynn. Note that the scatter in the data points for all the alloy systems is appreciable. Γ_{theor} is based upon our self-consistent calculations.

We further note from Table I that the influence of core electrons is consistent between the experimental values and the density-functional calculation, but is inconsistent with the asymptotic (phase shift) limit. Since Ge and Si both have a valence of 4, the difference in their fractional Knight shifts, i.e., $0.21 - 0.07 = 0.14$, is a measure of the core-electron contribution to the Knight shift. This value is the same as the measured fractional Knight shift due to Ga which is isovalent with Al. The density-functional calculation shows this same behavior, i.e., $\Gamma_{(32)\text{Ge}} - \Gamma_{(14)\text{Si}} = 0.44 - 0.29 = 0.15 \approx \Gamma_{(31)\text{Ga}}$, while the phase-shift calculation does not. This further points out the inconsistencies introduced by using even self-consistent phase shifts in trying to model phenomena where this asymptotic calculation is inappropriate.

We now comment on possible sources contributing to the apparent disagreement between theoretical and experimental results in Table I. We first discuss the shortcomings of our theoretical approach. In spite of the fact that the present calculations are the best to date, these shortcomings may include (1) other contributions such as core-polarization and orbital effects that can contribute to the fractional Knight shifts. In most simple metals, the core-polarization contribution is about 30% of the direct term.¹⁵ No calculations of this contribution in alloys are available to our knowledge. (2) We have assumed that Pauli spin susceptibility is the same in the imperfect metal as that in the perfect host. (3) We have neglected the effect of structural disorder on the electron-spin-density distribution. Corrections beyond the jellium model may be necessary. (4) The pair-correlation function $g(r)$ used in

our calculation is that for the perfect liquid metal. The presence of impurities in nondilute proportions may affect this assumption.

From the experimental view, as pointed out earlier, the shifts in the precession frequency due to impurities may be small and thus difficult to measure in very dilute alloys. The addition of large amounts of impurities may introduce complicating interactions between impurities and thus affect the measured fractional shift. To illustrate this point further, we show in Fig. 5 the experimental $\Delta K/K$ for various impurity concentrations in Al/Mg, Al/Ga, Al/Si, and Al/Ge alloys. These data were taken from the work of Rigney and Flynn.⁷ The straight lines are the fits to the data points used in Ref. 7. The slope Γ of these straight lines is the experimental values given in Table I. It is clear that the data points have considerable scatter in them and the slope of $\Delta K/K$ versus c can be easily altered. Thus it would be useful to have additional experimental studies of these systems, particularly at low concentrations. Until more accurate experimental values of Γ are available, it will be hard to judge the importance of various factors discussed in analyzing our theoretical results.

ACKNOWLEDGMENT

This work was supported in part by grants from the Thomas F. Jeffress and Kate Miller Jeffress Memorial Trust and by the National Science Foundation.

APPENDIX: PROCEDURE FOR NUMERICAL EVALUATION OF FRACTIONAL KNIGHT SHIFT

It was pointed out in the text that the contribution to fractional Knight shift, $\Gamma = K^{-1} \partial K / \partial c$, arises from host atoms at close proximity to the impurity (where perturbation is large, but number of host atoms small) as well as those at large distances (where perturbation is small but number of host atoms is large). Thus it is not only important to have a theory that is valid at all distances from the impurity, but also the contribution from all atoms should be calculated properly in numerical computations. In the following we provide details of our numerical approach and point out some of the difficulties inherent in the earlier approach of Rigney and Flynn.

For the density-functional calculations, the integral in Eq. (14) was divided into three regions, namely,

$$\begin{aligned} \Gamma = \frac{\Delta \bar{K}}{\bar{K}} \frac{1}{c} = & \int_0^{R_I} d^3 r \rho(r) \left[\frac{\Delta \tilde{n}}{n_0^\uparrow - n_0^\downarrow} \right] \\ & + \int_{R_I}^{R_{II}} d^3 r \rho(r) \left[\frac{\Delta \tilde{n}_{\text{asym}}}{n_0^\uparrow - n_0^\downarrow} \right] \\ & + \int_{R_{II}}^\infty d^3 r \frac{1}{\Omega_0} \left[\frac{\Delta \tilde{n}_{\text{asym}}}{n_0^\uparrow - n_0^\downarrow} \right]. \end{aligned} \quad (\text{A1})$$

In the self-consistent calculation of $\Delta \tilde{n}$, the density functional Eq. (16) was integrated from the impurity site to a maximum distance $R_I = 14.0a_0$ using a Herman-Skillman mesh. Thus the first term in Eq. (A1) was computed using self-consistent $\Delta \tilde{n}$ and $\rho(r) = \Omega_0^{-1} g(r)$ from Fig. 4. For the second term in Eq. (A1) we chose $R_{II} = 60.0a_0$ and fitted the spin density $\Delta \tilde{n}$ to an asymptotic formula for $r > R_I$,

$$\Delta \tilde{n}_{\text{asym}} = A \cos(2k_F r + \theta) / r^3. \quad (\text{A2})$$

The amplitude A and phase factor θ were determined by fitting (A2) to the last two points of our calculated self-consistent $\Delta \tilde{n}(r)$. In the third region $R_{II} < r < \infty$, we set $\rho(r) = \Omega_0^{-1}$ since $g(r) \rightarrow 1$ in this limit and the integration of the third term in Eq. (A1) is evaluated analytically. The fractional Knight shift using the asymptotic formula Eq. (27) was evaluated in a manner described above. The phase shifts δ_l in Eq. (27) were obtained from our density-functional calculation, namely $\delta_l = \delta_l^\uparrow + \delta_l^\downarrow$ for electrons at the Fermi surface. We retained partial waves $0 \leq l \leq 10$ in the summation in Eq. (27).

It is now appropriate to comment on the difficulties associated with the numerical procedure used by Rigney and Flynn to evaluate Eq. (28). First, these authors restricted the sum over partial waves to $0 \leq l \leq 2$. Since the deriva-

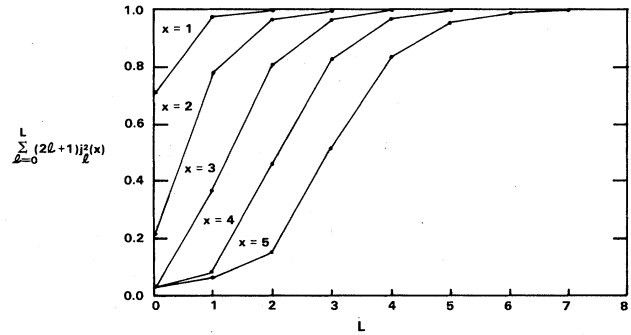


FIG. 6. Plot of $\sum_{l=0}^L (2l+1)j_l^2(x)$ vs L for various arguments of the Bessel functions. Note that the sum is independent of x only if it is carried to large values of L .

tion of Eq. (28) relies on the condition that the identity in Eq. (26) be satisfied, we show in Fig. 6 a plot of $\sum_{l=0}^L (2l+1)j_l^2(x)$ versus L for several values of x . For this sum to be independent of x , one has to sum over a large number of l values—the larger the x value, the greater the number of l values required in the sum to satisfy the identity in Eq. (26). Thus for impurities for which the scattering phase shifts for $l > 2$ are important, one has to include higher l terms in evaluating Eqs. (27) or (28). The second problem is associated with the evaluation of A_l 's and B_l 's in Eq. (29).

To derive the asymptotic behavior of the integrands in Eq. (29), we note that

$$j_l(x) \rightarrow \frac{1}{x} \cos \left[x - \frac{l+1}{2} \pi \right], \quad \text{as } x \rightarrow \infty, \quad (\text{A3})$$

$$n_l(x) \rightarrow \frac{1}{x} \sin \left[x - \frac{l+1}{2} \pi \right] \quad \text{as } x \rightarrow \infty.$$

Thus

$$[n_l^2(x) - j_l^2(x)] \simeq -\frac{1}{x^2} (-1)^{l+1} \cos 2x, \quad \text{as } x \rightarrow \infty, \quad (\text{A4})$$

$$[n_l(x)j_l(x)] \simeq \frac{1}{2x^2} (-1)^{l+1} \sin 2x, \quad \text{as } x \rightarrow \infty.$$

Since $\rho(r) \rightarrow \Omega_0^{-1}$ as $r \rightarrow \infty$, Eq. (29) in the asymptotic region would go as a sinusoidal function. Thus the A_l 's and B_l 's cannot be numerically evaluated. We therefore recommend the use of Eq. (27) for the asymptotic formula for the Knight shift.

*On leave of absence from Institute of Physics, Sachivalaya Marg, Bhubaneswar, Orissa, India.

¹W. D. Knight, Phys. Rev. **76**, 1259 (1949).

²C. H. Townes, C. Herring, and W. D. Knight, Phys. Rev. **77**, 852 (1950).

³P. H. Dederichs and R. Zeller, in *Point Defects in Metals II*, Vol. 87 of *Springer Tracts in Modern Physics*, edited by G. Höhler (Springer, New York, 1980).

⁴L. Schwartz and H. Ehrenreich, Ann. Phys. (N.Y.) **64**, 100 (1971); B. Movaghar, D. E. Miller, and K. H. Bennemann, J.

- Phys. F 4, 687 (1974).
- ⁵N. W. Ashcroft and J. Lekner, Phys. Rev. 145, 83 (1966).
- ⁶P. Hohenberg and W. Kohn, Phys. Rev. 136, B964 (1964); W. Kohn and L. J. Sham, *ibid.* 140, A1133 (1965); A. K. Rajagopal and J. Callaway, Phys. Rev. B 7, 1912 (1973).
- ⁷D. A. Rigney and C. P. Flynn, Philos. Mag. 15, 1213 (1967).
- ⁸M. Iwamatsu, R. A. Moore, and S. Wang, J. Phys. F 13, 503 (1983).
- ⁹R. L. Munjal and K. G. Petzinger, Hyp. Int. 4, 301 (1978).
- ¹⁰P. Jena, K. S. Singwi, and R. M. Nieminen, Phys. Rev. B 17, 301 (1978).
- ¹¹R. R. Fessler, R. Kaplow, and B. L. Averbach, Phys. Rev. 150, 34 (1974).
- ¹²O. Gunnarson, B. I. Lundquist, and J. W. Wilkins, Phys. Rev. B 10, 1319 (1974).
- ¹³M. Manninen, P. Jena, R. M. Nieminen, and J. K. Lee, Phys. Rev. B 24, 7057 (1981).
- ¹⁴J. Ziman, Philos. Mag. 6, 1013 (1961).
- ¹⁵N. C. Halder and P. Jena, Phys. Rev. B 4, 2385 (1971).